A new affordable and quick experimental device for measuring the thermo-optical properties of translucent construction materials

Ali Hamada Fakra, Blázquez Recio Alfonso José, Nour Murad, Jean Claude Gatina

A new affordable and quick experimental device for measuring the thermo-optical properties of translucent construction materials

Damien Ali Hamada Fakra[1,], Blázquez Recio Alfonso José[1], Nour Mohammad Murad[1], Jean Claude Gatina[1]

[a] *PIMENT Laboratory - University of la Réunion, 117 Rue du General Ailleret - 97430 Le Tampon - REUNION*
[b] *Escuela Tecnica Superior de ICCP - University of Granada, Calle Doctor Severo Ochoa, S/N- 18001 Granada -SPAIN*
[c] *Energy Lab (LE^2P) Laboratory - University of la Réunion, 40 Avenue de Soweto - 97410 Saint-Pierre - REUNION*

Abstract

The knowledge of thermo-optical properties of building materials is an essential factor for studying human comfort inside the building. Experiments are generally used to determine these properties. Each thermo-optical coefficients (i.e. the thermal conductivity, optical reflectance, transmittance and absorbance of the materials) can be measured separately by various devices. However, considering the new and complex materials that are emerging, for example, the translucent materials, the existing measuring instruments are finding it challenging to characterize these coefficients correctly. In this article, a new experimental device based on a spherical environment is proposed. The proposed system is capable of measuring the optical reflectance, transmittance, absorbance, and the thermal conductivity of homogeneous and innovative construction materials over a short experimental duration. The measurement protocol, the physical laws associated with the new experimental device, and the calibration tests of the measuring sensors are described. Furthermore, an application test based on a known reference, a polycarbonate construction material, is described in detail to prove the ability of the device to correctly measure these thermo-optical property coefficients. The results obtained show a relative error The results obtained show a relative error around of +/- 5%. Comparisons of the absolute error with the test results from the experimental device proposed by ASTM International (formerly the American Society for Testing and Materials) show that the maximum errors contributed by the new system described in this work to perform these measurements are generally acceptable. For the polycarbonate material, we obtained the following relative errors: 4.5% for the thermal conductivity, 4.7% for the optical reflectance, 0.56% for the optical transmittance and 1.78% for the optical absorbance.

Keywords:
Optical reflectance, Optical transmittance, Optical absorbance, Thermal conductivity, Low-cost device, Experimentation, Heat transfer, Polycarbonate

*Corresponding author

Table of contents

1. Introduction

Human beings have always researched to live in comfort whatever the environment that surrounds them. Even when it comes to shelter inside a building, this comfort pursuit has always been the top priority. That is why interior comfort indicators have been defined by civil engineers. Majority of these indicators are based on the knowledge of the thermo-optical properties of construction materials. In fact, understanding some properties of construction materials (i.e. thermal, acoustic, visual or even pollution-related phenomenon) is an essential factor for studying human comfort inside the building. These properties either make life inside a building comfortable or not. Visual comfort particularly needs quantitative indicators to judge whether a home is adequately lit to avoid either darkness or visual glare. Three coefficients are directly responsible for indoor visual comfort: optical reflectance, optical transmittance and optical absorbance of the material. It is also necessary to have physical variables to characterize the thermal insulation in a building to prevent the person inside from feeling too hot or cold (thermal comfort). One coefficient is particularly important: the thermal conductivity of the material. These indicators are related to the structure of the building materials used. Experiments on the construction materials generally determine the comfort indicators. Each thermo-optical coefficient can be measured separately using various devices. However, considering the new and complex materials that are emerging, like translucent materials among others, the existing measuring instruments find it challenging to characterize them correctly. Moreover, the specific and high cost sensors are incapable of measuring the thermo-optical coefficients simultaneously.

With the discovery of new and much more sophisticated building materials (i.e., phase change materials, translucent materials, thin reflective products, etc.), the measurement of thermo-optical properties, such as the optical absorbance, reflectance, transmittance, and thermal conductivity of such materials, is becoming increasingly complicated. Existing devices do not take into account certain complex phenomena related to the nature of the material. Additionally, the high costs associated with designing these measuring devices considerably slow the progress needed to standardize new experimental methods capable of truly considering the heat transfer phenomena of such innovate materials. Accordingly, a technique that can achieve the simultaneous measurement of these four coefficients on a single machine must be developed. This article responds to the three abovementioned problems. An inexpensive experimental device has been designed to measure all four thermophysical coefficients (i.e., transmittance, reflectance, absorptance, and thermal conductivity) of complex construction materials. The following steps have been taken to achieve this objective:

- The first step was to design the system from less expensive materials, imagine the principal light source (i.e., monochromatic) and choose the measurement sensors and their positions in the measurement system;

- The second step was to define the laws associated with the thermal phenomena of the system, the source, and the measurement sensors used;
- The third step was to establish a measurement protocol and then test the reliability of the system to measure the four thermo-optical coefficients of a complex construction material based on measurement standards [**?** **?**].

2. State-of-the-art measurement methods

The techniques employed to measure radiative fluxes by thermal heat transfer and optical phenomena (photometric energy transfer, also known as luminous fluxes) for a given wavelength are similar. The main aspect that differentiates these techniques is the type of measurement sensor used: on one hand, a fluxmeter (generally called a radiometer) is used to measure radiative fluxes in Wm^{-2}; and on the other hand, a luxmeter (generally called a photometer) is used to measure artificial lighting or daylighting fluxes in Cdm^{-2} (or in lux). A summary of the existing techniques capable of measuring thermal radiation in the visible and IR environment (i.e., the case of interest herein) is presented below.

2.1. Measurement of reflectance (ρ)

Reflection of heat is the process by which a fraction of the radiant flux incident on a surface is returned into the same hemisphere whose base forms the surface that contains the incident radiation. The general definition of reflectance (ρ) is the ratio of the reflected radiant flux (ϕ_ρ) to the incident radiant flux (ϕ_i) given by (**??**).

$$\rho = \frac{\phi_\rho}{\phi_i} \tag{1}$$

Several forms of reflectance can be measured separately: total, diffuse, specular, or coherent [**?**]. Some reflectances are simple to measure [**?** **?** **?** **?** **?**], whereas others are relatively difficult to measure [**?**]. The first reflectometer dates back to 1938 [**?** **?**]. Some of the existing reflectometers are specifically dedicated to the measurement of normal incident radiation [**?** **?**]. The corresponding measurement and acquisition techniques are described in [**?** **?** **?** **?**]. Many studies have been performed on angle resolved measurements based on hemispherical systems [**?** **?** **?** **?** **?** **?** **?** **?** **?**]. Most of these devices are designed on the basis of integrating spheres (see the state-of-the-art methods for measuring transmittance in section **??** for more details). Numerous studies on the general theory of integrating spheres have thus been conducted to enable these measurements [**?**]. Integrating spheres are most commonly used when taking specular and diffuse flux measurements of a material (specimen) in the visible or near-infrared spectral range [**?** **?** **?** **?** **?** **?**]. Many articles have been published to thoroughly explain the instrumentation, method, and procedure related to the measurement of the reflectance of a material installed in an integrating

sphere [? ? ? ? ?]. The use of integrating sphere methods to measure the optical properties of solar energy materials and solar cells is illustrated in the works of A. Parretta et al. [? ? ? ? ? ? ? ?]. Thanks to these experimental devices, it is possible to measure the diffuse and specular reflectance separately, and the sum of these two reflectances constitutes the total reflectance of the material. Several sample positions in integrating spheres have been proposed in previous studies [? ? ? ?]. Alternatively, other forms of measurement systems have been proposed as substitutes in the literature when the configuration of the integrating sphere does not allow the reflectance to be measured; these alternatives take specular hemispherical, paraboloidal, and ellipsoidal forms [? ? ?]. The energy source used in these experiments is generally monochromatic and coherent, such as a laser (see the literature for more information on the subject [? ? ?]). Other laboratories prefer to use a goniometer to measure the BRDF (i.e. Bidirectional Reflecting Distribution Function) [?]. The methods for measuring the reflectance are described in [? ? ?]. Several shape configurations, as well as the ideal color of an integrating sphere, have been discussed in the literature [? ?]. The mixture of barium ($BaSO_4$) additive with the product that will be used for painting inside the sphere makes it suitable to produce a high reflectance inside the sphere. Barium is generally a white powder and can be used in optical applications because of its relatively constant spectral reflectance ranging from ultraviolet to infrared wavelength. Barium sulfate exhibits a diffuse reflectance characteristic and is resistant to high-intensity optical radiation. We obtain a solution in the form of paint by mixing barium sulphate and water. This paint can be used as a coating to diffuse reflectance plates and integrating spheres. The typical high reflectance value of barium sulphate solution is 99% in the visible spectrum between 380 nm and 780 nm. The best material used for reflectance standards is the Spectralon®, produced by Labsphere. A detailed description of the characterisation of these standards can be found in [?]. Many documents on the manufacturing, calibration, and characterization of the reflectance of a specimen are available in [? ? ?].

2.2. Measurement of transmittance (τ)

The transmission flux is used to describe the process by which incident radiant flux leaves a surface from a side other than the incident side, usually the opposite side. The transmittance (τ) is the ratio of the transmitted flux (ϕ_τ) to the incident flux (ϕ_i) given by (??).

$$\tau = \frac{\phi_\tau}{\phi_i} \tag{2}$$

Researchers generally employ a spectrometer to measure the transmittance coefficient [? ?]. The source used in most experiments is a monochromatic light (e.g., a laser). Since 1972, many measuring devices based on this technique have been developed [? ? ? ? ?], most of which utilized an integrating sphere system ([? ? ? ?]). The reliability and robustness of these experimental devices and the measurement methods used are detailed in the literature [? ? ? ? ? ?]. For more information about the spectrometer system, see [?].

Currently, many laboratories are conducting joint studies to compare the different transmittance measurement methods proposed in many countries.

2.3. Measurement of absorptance (α)

The definition of absorption is the process by which incident radiant flux is converted into another form of energy, usually heat. The absorptance is the fraction of incident flux that is absorbed. The absorptance (α) of an element is defined by (**??**):

$$\alpha = \frac{\phi_\alpha}{\phi_i} \tag{3}$$

The absorption of a construction material is generally not measured because the errors generated by the experimental devices utilized to characterize the absorptance are very high. Several laboratories prefer to apply indirect measurements to obtain this physical property (i.e., to deduce the value of the absorptance from measurements of other measurable thermo-optico-physical variables). In fact, it is easier to derive the absorptance from the law of energy conservation given by equation (**??**).

2.4. Measurement of thermal conductivity (k)

The thermal conductivity (k) characterizes the amount of heat required per m^2 for 1 m of a homogeneous material to obtain a temperature difference of 1° between two sides over a unit of time. The thermal conductivity is an intrinsic property of a material that varies according to the temperature at which the measurement is carried out. Measurements are usually conducted at 300 K to facilitate the comparison of some elements with others. When the specimen is not homogeneous (i.e., when it is heterogeneous but uniformly distributed), a useful value of the thermal conductivity is obtained in the laboratory as a weighted average of the coefficients of each material.

Ref. [**?**] emphasized the use of only one physical parameter, the thermal conductivity, in design, construction and evaluation based on the ASTM E1225 standard [**?**]. The methods for measuring thermal properties are divided into two groups [**?**]: steady methods and dynamic methods. Dynamic methods do not need to reach a steady state and are therefore faster than steady methods; however, dynamic methods are more difficult to apply. In our work, we use the steady method based on a Peltier plate heat source. The ASTM E1225 standard describes a technique for determining the thermal conductivity of homogeneous isotropic solids using a comparative heat flux meter. This technique can determine the thermal conductivity in the approximate range from 0.2 to 200 $Wm^{-1}K^{-1}$ over a temperature range between 90 and 1300 K (or from -183° to 1026°) but the precision of this method is not sufficient. Other methods and processes exist for measuring thermophysical properties. For example, Ref. [**?**] described a quantitative thermography technique that is currently accepted as a reliable method for measuring the thermal transmittance and thermal conductivity of opaque elements.

It has been more than fifty years since Parker et al. [**?**] released their original paper introducing the flash technique. Since then, this photothermal experimental method has been extended worldwide and has become the most popular approach for measuring the thermal diffusivity and thermal conductivity of solids. The simplicity and efficiency of the measurement process, the accuracy and reliability of the results, and the possible applications under a wide range of experimental conditions and materials are the main advantages of this method. The flash method has become the standard in many countries, which is evidence of its universality [**?**].

3. Materials and method

3.1. Description of the new double integrating sphere device

The initial configuration of the prototype is based on the one developed by Parretta in 2007 [**?**] denoted as double-cavity radiometer (DCR) (see Figure **??** and **??**).

Parretta et al. [**?**] developed a radiometric method suitable for measuring both the total power and the flux density profile of concentrated solar radiation. The high-flux density radiation is initially collected by the first optical cavity where it is integrated, after which it is driven and attenuated into the second optical cavity, where it is measured by a conventional radiometer operating under a stationary irradiation regime. The attenuation factor is regulated by properly selecting the aperture areas between the two spherical cavities.

Parretta device has been designated to characterise a concentrated solar beam. In this article, the newly developed design for measuring the optical and thermal properties of materials has taken inspiration from Parretta's device.

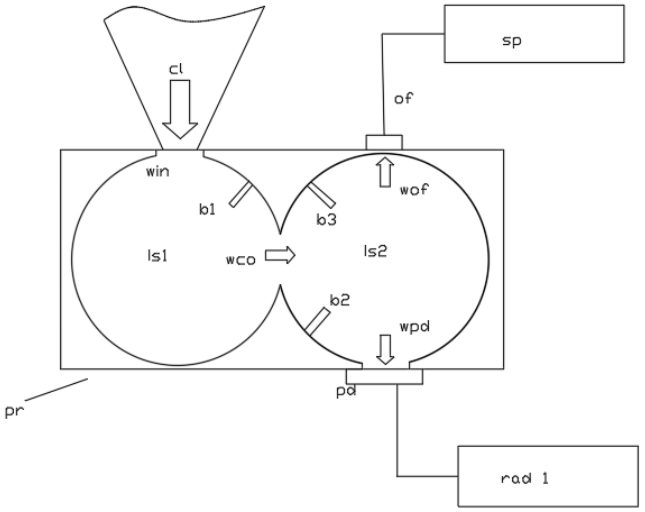

Figure 1: Schematic of the DCR (double-cavity radiometer) [**?**] for kind permission of A. Parretta

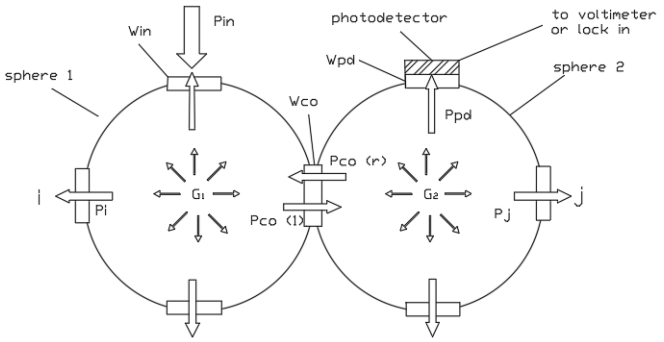

Figure 2: General radiation transfer schematic of the radiometer with two coupled integrating spheres [**?**] for kind permission of A. Parretta

Taking advantage of this two-sphere configuration to transmit fluxes, other authors began to improve upon this idea to develop instrumentation.

In this work, the article of Chong [**?**] is of special importance. An optical scanner capable of acquiring the flux distribution pattern of a light source on a 2D flat surface was designed and built; for this purpose, 25 single-row photodiodes with fixed distances that can scan and acquire flux distribution data in a 2D measuring plane were used. The research of Morales [**?**] was also of special relevance, as the locations of the detectors were reduced to 3 optimal places.

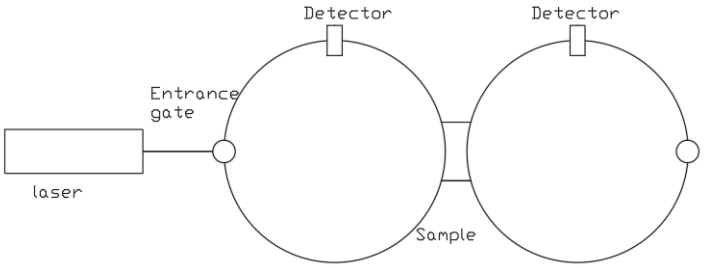

Figure 3: Integrating spheres [**?**]

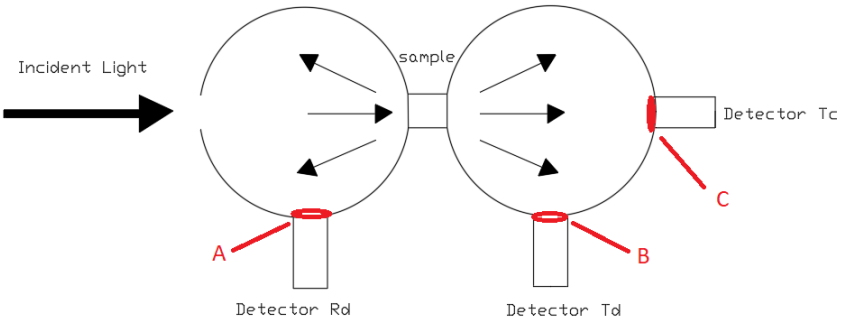

Figure 4: Double integrating sphere arrangement for the simultaneous measurement of the reflectance (one sensor in position A) and the transmittance (two sensors in position B and C) for a given specimen material (see [**?**])

An integrating sphere with a diameter of 5.08 cm and 1.27 cm ports (i.e. openings) was used in Salas Master degree in research (see [**?**]). This integrating sphere is made of a material commercially known as Spectralon®, which as previously discussed, is famous for having the highest diffuse reflectance of all known materials (it is capable of reflecting 99% of incident light in the range of 200-1100 nm); in addition, this material is highly Lambertian. Salas [**?**] also used a He-Ne laser with a power of 12 mW, but to adapt it to more materials, the power must be increased. The material should be larger to measure its thermal conductivity. Upon examining the results obtained in the above-mentioned thesis, spheres with a diameter of 30 cm and a laser with a power reaching up to 200 mW were used.

Having described the design of the device, the particular design of this study will be introduced as well as the dimensions and materials used.

3.1.1. Integrating spheres

To construct the integrating spheres, two spheres of 30 cm in diameter obtained from the lampshades of the luminaries were used. A detailed description on how to build a low cost integrating sphere from garden lamps can be found in the chapter 13 of ref. [**?**].

The problem with these spheres is that they are made of a translucent plastic material. This is evident, as they were designed to transmit fluxes (light and thermal heat) from the interior to the exterior.

It is therefore important to limit the exchange of heat flow between the interior of the spheres and the external environment. It is also essential that the flows conveyed inside the spheres should not be able to propagate towards the outside.

To solve this problem, the outer surface was painted Matt black and the inner surface Matt white so that the sphere resembles an inner Lambertian surface as much as possible. In this condition, the opacity of the sphere could also be obtained. Concerning heat transfer, a protocol for excluding radiation fluxes (i.e., exterior fluxes penetrating inside the sphere during the experiment) will be presented. For further details about this protocol, see section **??**.

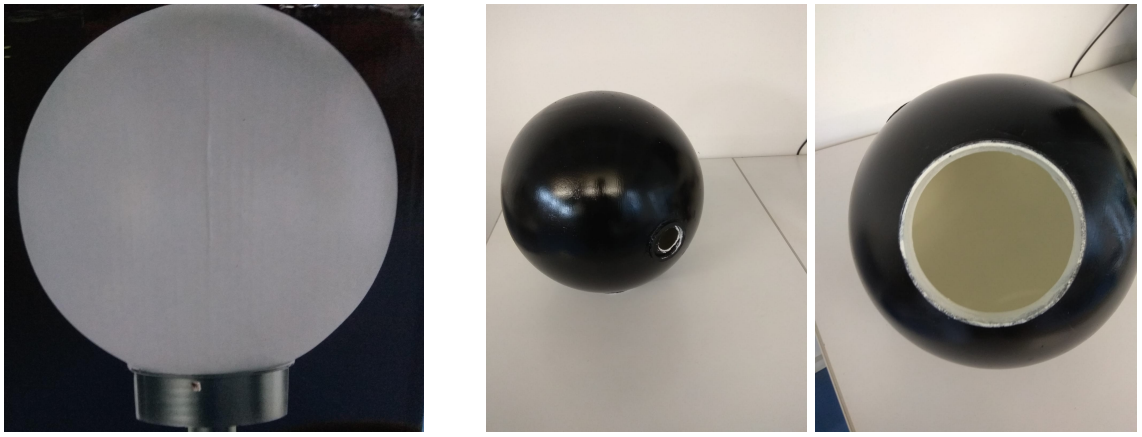

(a) **b)**

Figure 5: Sphere using in the experimentation: (a) Unpainted sphere ; (b) Painted integration spheres: white inside and black outside

3.1.2. Light source

For the thermal flux emission source, we selected a red monochromatic laser ($\lambda = 650mm$).The output power is approximately 200 mW (Class 3B). The laser source adopts a common USB interface, a polymer battery and an imported metal module (see Figure **??**,a. for the form).

(a) **(b)** **(c)**

Figure 6: Supports: (a) Laser form; (b) Laser support and (c) Sphere support

For more information about the technical details of the laser, see appendix A.

3.1.3. Supporting and finishing parts

As we can see in Figure **??**,a., by removing the lower part of the sphere (where the lamp is originally housed), we have an opening 11.5 cm in diameter. A piece with a regular internal surface has been reproduced by a 3D printer that can be inserted where the lamp used to be (see Figure **??**,c.). These pieces have been painted Matt white on one side and Matt black on the other to avoid transmittance fluxes.

To achieve mechanical stability, cylinders of 5.5 cm height and 11 cm diameter were reproduced by means of a 3D printer and attached to the lower part of the sphere. These cylinders are characterized by having a small ring with a height of 0.5 cm in their lower parts that will later be used to create rails to move the spheres (see the rail in Figure **??**,a.).

To move the laser to the correct position, a support was built (see Figure **??**,b.) using a 3D printer.

3.1.4. Specimen support

By means of the abovementioned 3D printer, five cylinders with an outer diameter of 5.5 cm and an inner diameter of 4.5 cm have been manufactured with different heights depending on the samples to be studied: 1 cm, 0.8 cm, 0.6 cm, 0.5 cm and 0.2 cm (see Figure **??**). These cylinders are white to reflect any flux that could be produced inside. The cylinders are placed to connect the two spheres, allowing the beam from the laser to directly impact the specimen.

Figure 7: Specimen support

The diameters of the cylinders were calculated to facilitate the measurement of the thermal conductivity, as we will see in section **??**. The specimens used in the experiment have identical diameters (i.e., approximately 3.5 cm). The diameter of the cylinder sample holder is larger than that of the specimen (i.e., interior diameter equal at 3.49 cm and exterior 4.5 cm, for 0.5 cm thickness). The contact position of the two spheres with the cylinder sample holder were established by means of two others fixed cylinders in the exterior surfaces of the spheres (see Figure **??**). The height of the cylinder sample holder varies as function of the thickness of the studied sample. First, the sample is joined to the cylinder sample holder, then the cylinder sample holder is tightened to the fixed cylinder on the two spheres.

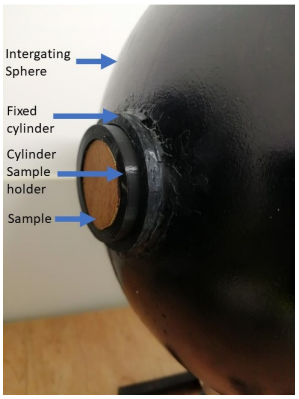

Figure 8: Contact between sample, cylinder sample holder, fix cylinder and opening spheres

3.1.5. Source of hot and cold radiation fluxes

To measure the thermal conductivity of a material, it is necessary to have a source of both hot and cold radiation fluxes to generate a thermal flux between the surfaces. Two Peltier plates (model TEC1-12706, see appendix B for more information) are available for this purpose. Figure **??** shows the location of the thermal conductivity k value measurements. When these plates are connected to a power supply, one of their surfaces cools down, whereas the other heats up. The dimensions of the Peltier plates are 4 cm x 4 cm, so the specimens must be smaller than this area to obtain a uniform flow; the specimen support is calculated accordingly. To dissipate heat from the plates, a heat sink is deployed (see Figure **??**).

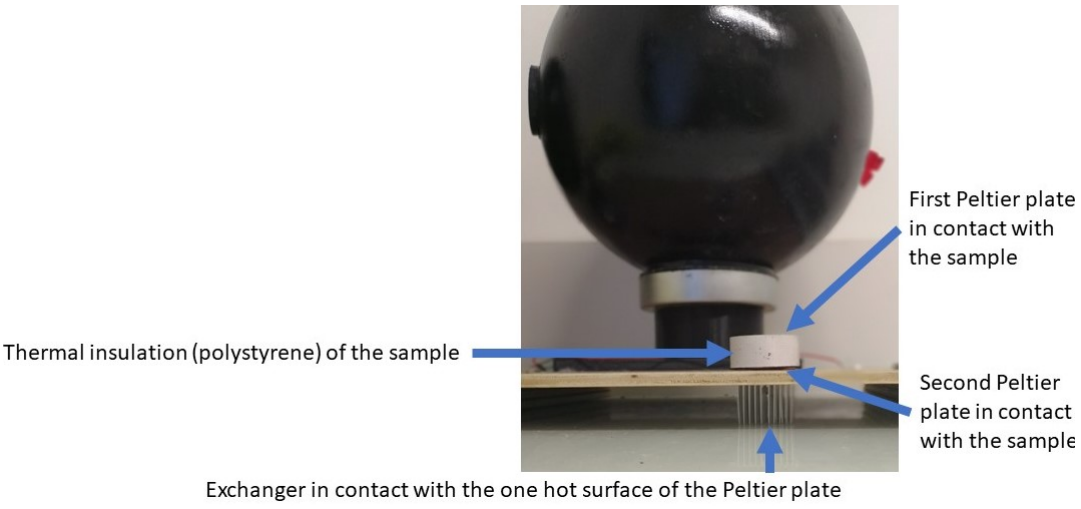

Figure 9: Thermal Conductivity measurements k location

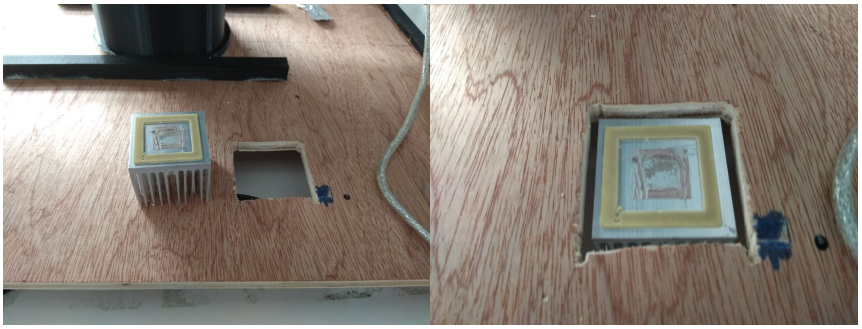

Figure 10: Heat sink

3.2. Measurement of optical reflectance (ρ), transmittance (τ), and absorbance (α)

The integrating sphere devices have been built with materials that generate Lambertian surfaces [**?**], that is, surfaces that reflect radiation fluxes in a diffuse manner (see Figure **??**,b.) and whose intensity distribution of the reflected flux obeys Lambert's cosine law, given by the following relationship:

$$I_r(\theta) = I_0 cos\theta \tag{4}$$

where I_r is the reflected radiant intensity expressed in W/sr, I_0 is the radiant intensity of the radiation reflected at $\theta_0 = 0^o$ and θ is the angle measured from the normal. Figure **??**,a. shows the radiant intensity distribution generated by a Lambertian surface. Another way of defining a Lambertian surface is to say that its radiance L in $Wsr^{-1}m^{-2}$ is constant, that is independent on the observation angle θ.

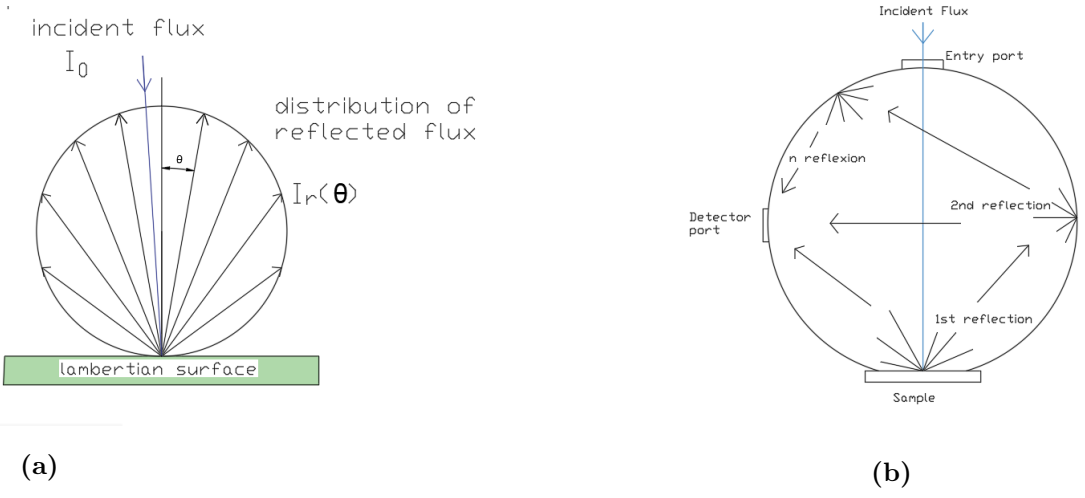

Figure 11: Reflections phenomena within the sphere: (a) Model of reflected flux a Lambertian surface / (b) Multiple reflections in an integrating sphere

The standards of diffuse reflectance, like those realised by $BaSO_4$ coating or by Spectralon® (Labsphere) do not behave as perfect Lambertian diffusers. To better understang how they differ

from an ideal Lambertian diffuser, see the work of Parretta [**?**].

Assuming that the integrating sphere has Lambertian walls, the incident flux to the sphere is reflected several times such that the incident flux is homogeneously distributed over the entire surface of the sphere (an ideal integrating sphere reflects the incident flux entirely; spheres of higher quality reflect approximately 99% of the flux in relation to the design wavelength range). Energy irradiance is defined as the radiant flux per unit of irradiated area (see Equation (**??**)).

$$E = \frac{\Phi}{A} \tag{5}$$

where ϕ is the radiant flux whose unit is the Watt (W) and A is the surface irradiated by the radiant flux in square meters (m^2). Therefore, the irradiance has power units on the surface units.

The total flux incident on the surface of the integrating sphere can be calculated in a very simple way because the irradiance is homogeneous. The irradiance on a detector placed in one of the openings of the sphere will be equal to the irradiance on the whole integrating sphere:

$$E_{sphere} = E_{detector} = \frac{\phi_{detector}}{A_{detector}} \tag{6}$$

and thus:

$$\phi_{sphere} = \phi_{detector} \frac{A_{sphere}}{A_{detector}} \tag{7}$$

where ϕ_{sphere} is the flux contained within the sphere, $\phi_{detector}$ is the flux in the detector, A_{sphere} and $A_{detector}$ are the areas of the sphere and the detector, respectively, where $A_{sphere} = 2\pi R^2$.

The flux contained in the sphere will be greater than the incident flux. The radiant flux contained within the sphere is higher than the incident flux because the incident flux undergoes multiple reflections within the sphere, which is more obvious if the contributions from each reflection are summed up. This fact is made explicit by the introduction of the concept of "sphere multiplier" [**?**].

For the first reflection, the reflected flux is:

$$\phi_1 = \phi_i \ \rho \tag{8}$$

Where ϕ_i is the incident radiant flux and ρ is the reflectance of the sample. The quantity f as the fraction of ports area is expressed as:

$$f = \frac{A_{doorSphere} + A_{doorDetector}}{A_{sphere}} \tag{9}$$

Here, $A_{doorSphere}$ is the entry port area, $A_{doorDetector}$ is the detector port area, and A_{sphere} is the surface of the integrating sphere. In the second reflection, the reflected flux is:

$$\phi_2 = \phi_i \rho \rho_w (1 - f) \tag{10}$$

Where ρ_w is the reflectance of the internal wall of the sphere. The reflectance of the detector was assumed negligible, whereas the reflectance of the entry port is naturally zero. The sample area was also neglected. The third reflection presents:

$$\phi_3 = \phi_i \rho \rho_w^2 (1-f)^2 \tag{11}$$

and so on until the n-th reflection, whose contribution is:

$$\phi_n = \phi_i \rho \rho_w^{n-1} (1-f)^{n-1} \tag{12}$$

By adding all these contributions, the flux integrated by the sphere after n reflections becomes:

$$\phi^n_{sphere} = \phi_i \rho + \phi_i \rho \rho_w (1-f) + \phi_i \rho \rho_w^2 (1-f)^2 + ... + \phi_i \rho \rho_w^{n-1} (1-f)^{n-1} = \phi_i \rho \sum_{k=0}^{n-1} \rho_w^k (1-f)^k \tag{13}$$

By stretching n to infinity, we finally have:

$$\phi_{sphere} = \phi_i \frac{\rho}{1-\rho_w(1-f)} \tag{14}$$

Now, by erasing the reflectance in terms of the flux, the following can be obtained:

$$\rho = \frac{\phi_{sphere}}{\phi_i}[1-\rho_w(1-f)] \tag{15}$$

For the flux passing through the sample to the second integrating sphere (see Figure **??**), we have:

$$\phi_{sphere2} = \phi_\tau \frac{\rho}{1-\rho_w(1-f)} \tag{16}$$

Where $\phi_{sphere2}$ is the radiant flux contained within the second integrating sphere and ϕ_τ is the flux transmitted by the sample. From Eq.**??** we obtain from the transmitted flux:

$$\phi_\tau = \phi_{sphere2} \frac{1-\rho_w(1-f)}{\rho} \tag{17}$$

Assuming again that the irradiance is homogenous at any point of the second integrating sphere, the total flux rate contained in the sphere can be written as a function of the flux rate on the detector mounted therein:

$$\phi_{sphere2} = \phi_{detector2} \frac{A_{sphere2}}{A_{detector2}} \tag{18}$$

By matching the two previous equations, the following is obtained:

$$\phi_\tau = \phi_{detecteur2} \frac{A_{sphere2}}{A_{detecteur2}} \frac{1-\rho_w(1-f)}{\rho} \tag{19}$$

When some of the photons incident on the sample are not absorbed or reflected by the material, they will pass through the sample and follow the same direction of propagation as the incident

beam if allowed to propagate freely. The radiant flux composed of these photons is called the coherent flux, and we represent it with $\phi_{\tau coherent}$.

With incident fluxes, it is simple to obtain the diffuse and coherent transmittances. Finding these transmittances is achieved by the following equations:

$$\tau_{diffuse} = \frac{\phi_\tau}{\phi_i} \tag{20}$$

$$\tau_{coherent} = \frac{\phi_{\tau coherent}}{\phi_i} \tag{21}$$

where $\tau_{diffuse}$ is the diffuse transmission and $\tau_{coherent}$ is the coherent transmission.

Knowing the reflectance and transmittance, it is possible, thanks to the energy conservation argument, to know the absorptance of the medium. Thus, the sum of the transmitted, reflected and absorbed fluxes must be equal to the incident flux and is given by:

$$\phi_i = \phi_{reflected} + \phi_\tau + \phi_{\tau coherent} + \phi_\alpha \tag{22}$$

By dividing everything by ϕ_i, we have:

$$1 = \rho + \tau_{diffuse} + \tau_{coherent} + \alpha \tag{23}$$

where α is the absorbtance of the medium. From this equation, it is possible to determine the absorption coefficient and the extinction coefficient of the material studied. Another technique for measuring the extinction coefficient of a material is ellipsometry. This technique allows the use of a model to determine the complex refractive index of a material as a function of its reflection coefficients and the phase change of the flux reflected from the surface of the material.

3.3. Fourier's law under steady-state conditions to determine k

The techniques for measuring the thermal conductivity of a material differ depending on the method employed to measure the surface temperature of the material and the type of contact (fluid-solid or solid-solid) selected for the surface measurement. Heat transfer is defined as the energy interaction caused solely by a temperature difference. Heat fluxes are a function of temperature differences, thermophysical properties, dimensions and geometries, time, and fluid flow. Heat transfer processes are classified into conduction, convection and radiation. Conduction is the transfer of energy from the most energetic particles to less energetic particles within a substance (solid, liquid or gas). In the presence of a temperature gradient, heat will flow from a high-temperature region to a low-temperature region. The heat flux transferred by conduction q_c (Wm^{-2}) is given by Fourier's law in Equation **??**.

$$q_c = -k.gradT = -k\frac{T_2 - T_1}{L} \tag{24}$$

where the temperatures T_2 and T_1 are measured at a distance L. The k parameter, expressed in $Wm^{-1}K^{-1}$, is a constant and represents a heat transport property known as thermal conductivity. Thermal conductivity is an inherent characteristic of a material and indicates its heat conduction capacity. A high thermal conductivity indicates that the material is a good conductor of heat, while a low thermal conductivity indicates that the material is a thermal insulator, i.e., a poor heat conductor.

3.4. Experimentation and Metrology

3.4.1. Flux sensors used in the experimentation and calibration tests

Measuring heat flow from conventional sensors on a curved surface (inside an integrating sphere) is very complicated. Therefore, an original solution is proposed: to install microscopic photodiodes capable of assuming the same role as a conventional fluxmeter. For this reason, 3 silicon PIN photodiodes (see Figure **??**) have been used as thermal flux detectors. To use these sensors, they first had to be calibrated with a reference fluxmeter; additionally, by means of the laser employed in the experiment, it is possible to convert mV to Wm^{-2}.

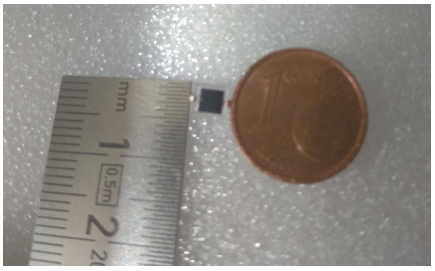

Figure 12: Silicon PIN photodiode

To calibrate the silicone PINs, a fluxmeter (calibrated using the same reference sensor) is used. The fluxmeter and two PINs were first placed inside a box measuring 30 cm high. The inside was lined with a white paper to make it somewhat similar to our model. The laser was placed in the upper part, and the box was closed. The laser was left on, and in the last two and a half minutes, the intensity of the laser dropped from 200 mW to 0 mW; we used this range for our calibration (see Figure **??**).

A calibration factor of 2.671 was obtained between the reference fluxmeter and the PIN for the range between 0 and 127 mW (see Figure **??**). The maximum value of the photodiode corresponded to 360 mV (approximately 127 mW in the fluxmeter), and the minimum value was 60 mV (corresponding to the offset of the sensor).

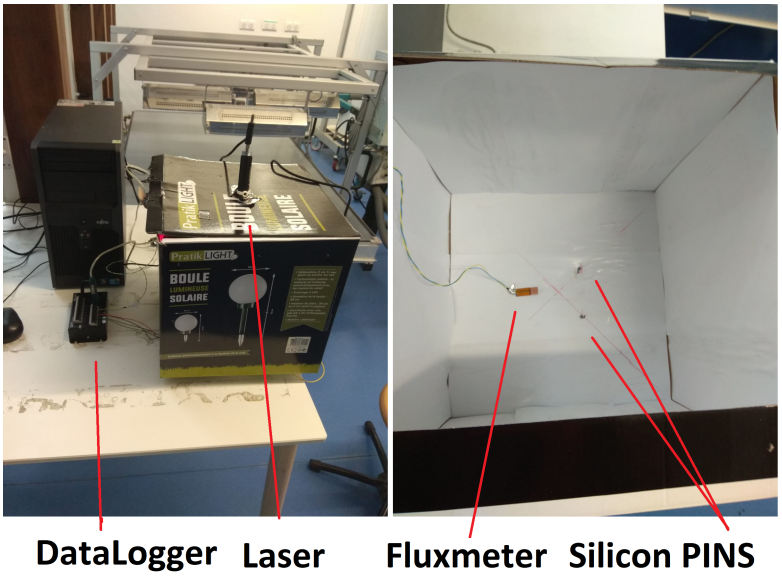

Figure 13: Calibration test of a silicon PIN

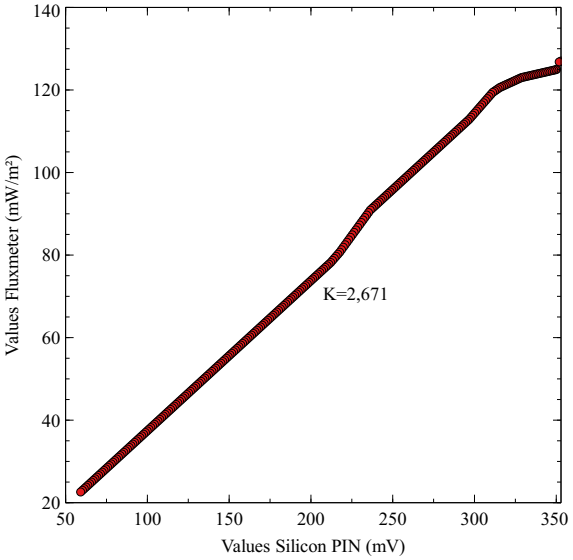

Figure 14: Comparison of the values between the fluxmeter (in mWm^2) and the photodiode PIN (in mV)

A value of 0 is not reached in this calibration because the photodiode is very sensitive, and when the laser is turned off, the PIN is able to sense the external radiation flux and the internal temperature.

3.4.2. Temperature sensors : calibrating the type K thermocouples

To calibrate the thermocouples, a EUROLEC thermostat (model CECS3) (see Appendix C for more information) was used; the thermocouples were calibrated before being used to measure the temperature (See Figure **??** for the data acquisition environment and Figure **??** for the results of

calibrations tests).

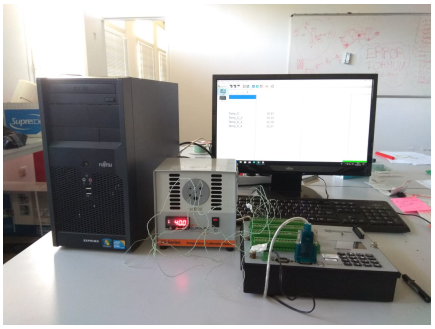

Figure 15: Data acquisition for the calibration tests

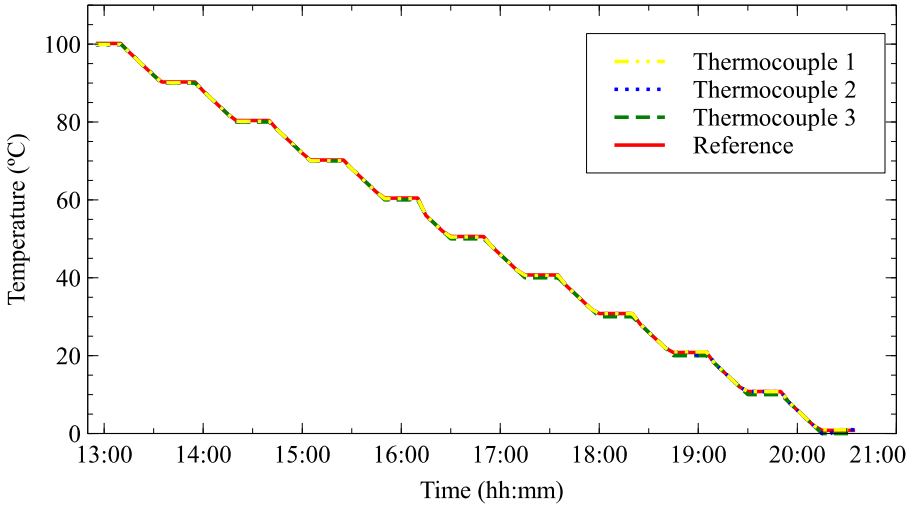

Figure 16: Calibration of the thermocouples

The two thermocouples used to conduct the thermal conductivity experiments have relative errors lower than 0.9%.

3.4.3. Heat flux source: Peltier plate material

The next step is to position the specimen on top of one of the Peltier plates without taking it out of the support (attaching a type K thermocouple on both plates) and coating the specimen with a polystyrene ring to achieve greater insulation. Figure **??**,a. and Figure **??**,b.,c.,d. show the positions of the type K thermocouples and the two Peltier plates used in the experiments and the thermal insulation around the specimen composed of the construction material.

The other Peltier plate is placed on top to generate a heat flux, and both plates are connected to generators with different voltages and intensities depending on the specimen (see Figure **??**).

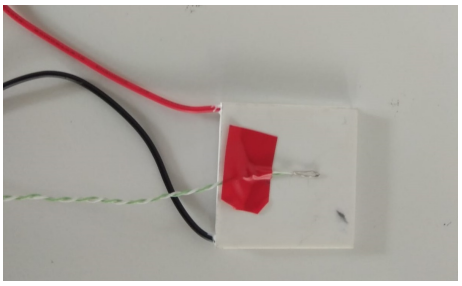

(a) Peltier plates with K type thermocouple

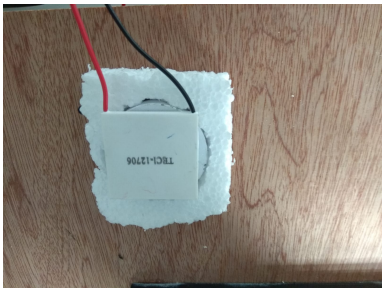

(b) Upper Peltier plat

(c) Isolation specimen (polystyrene)

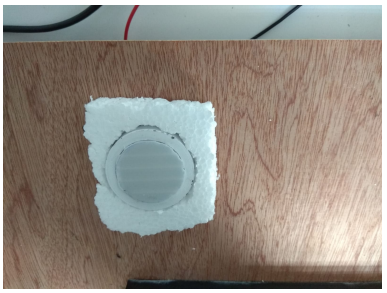

(d) Specimen surrounded by polystyrene

Figure 17: Thermal conductivity measurements

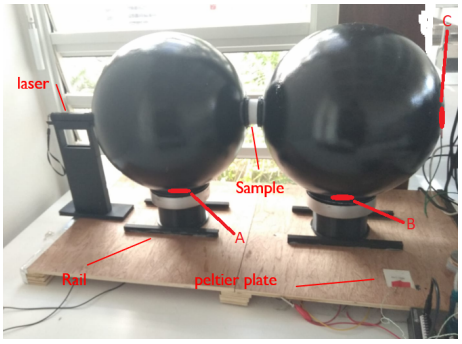

(a) Final assembly of the McM (multi-Coef-Meter) device

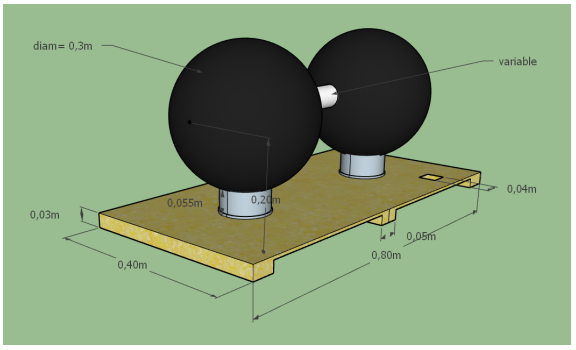

(b) Dimensions of the constructed prototype

Figure 18: The Multi-Coef-meter (i.e., McM device)

3.5. Description of the new measuring device: Multi-Coef-Meter (i.e. McM)

Finally, Figure **??** shows the prototype McM proposed in this work for measuring the 4 thermophysical properties of building materials. In this image, the sensors (i.e., photodiode PINs) positioned at points A, B and C (See Figure **??** for the sensors positions) measure the reflected flux ($\phi_{reflected}$), the diffuse transmittance flux (ϕ_{τ}), and the coherent transmittance flux ($\phi_{\tau_coherent}$) of the studied specimen, respectively. The positions of the photodiode PIN sensors (i.e., A, B and C) are shown in Figure **??**,a. The dimension of the McM device are reported in Figure **??**,b.

The techniques for measuring the thermal conductivity of material are different depending on the method of measuring the surface temperature of the material and the type of contact selected for the surface measurement (fluid-solid or solid-solid). In this article, the technique followed is the transient plane source (TPS). See the work of ASTM organisation [**?**] and Manetti [**?**] for

more information's about the technique for the measurements.

Let D and F (see Figure **??**) be two Peltier plates with known properties (see Appendix B). Let E be a specimen for which we are trying to determine the thermal conductivity k_x knowing its surface A_x and its thickness d_x. The measurement technique consists of sandwiching the sample E to be studied (see Figure **??**) using the other two Peltier plates D (hot source with temperature T_1 for example) and F (constant cold source with temperature T_2 for example) with constant flux. To maintain the constant flux at the surfaces of each Peltier plates in contact with the sample, constant temperature is needed, therefore, constant power. This constant flux passes through the specimen (see Figure **??**). The constant flux is used to deduce the value of the thermal conductivity of specimen E from the following relationship (conservation of the flux by the Fourier law in the steady state with the conduction heat exchange):

$$\phi = k_x \; A_x \; \frac{T_2 - T_1}{d_x} \tag{25}$$

The relation (**??**) is used to determine the thermal conductivity value k.

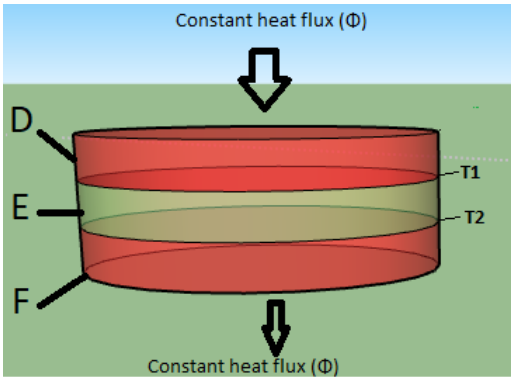

Figure 19: TPS (Transient Plane Source) method illustration

The specimen is insulated by polystyrene to neglect the influence of the cross-flow (i.e. horizontal or radial flux) in regards to the downward flux (vertical or descendant flux) of the measurement.

4. Applications to polycarbonate and other construction materials (validation of the new device)

4.1. Specimen tests

To confirm the reliability and functionality of the proposed McM device, we compared three different types of homogeneous samples, as shown in Figure **??**, whose thermal properties we already know: iron (solid grey color), wood (red color) and polycarbonate (white color). This comparison was also intended to classify polycarbonate from among two types of building materials: one has intermediate conductive properties (wood) and another that efficiently conducts heat (iron).

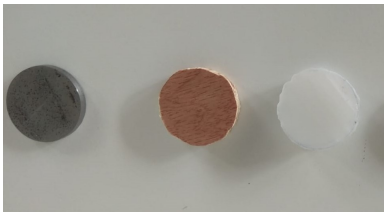

Figure 20: Specimen tests: iron, wood, polycarbonate

The exact dimensions and thermo-optico-physical properties of each specimen test are given in Tables **??**, **??** and **??**. The only fixed dimension to respect during the experiment in the McM (i.e. Multi-Coef-Meter device) is the diameter of the sample (i.e. 0.04 m). As far as thickness is concerned, it is possible to vary from 0 to 0.20 m (i.e., by moving the two spheres of the device apart).

4.2. Conditions of the experiments

Each sample was placed in the specimen support with the sizes described in **??** and then placed between the two spheres and in the path of the laser; then, measurements of the silicon PIN (which we placed in the position shown in Figure **??** before and after actuating the laser) were taken to determine how much radiant flux of the laser was transmitted, absorbed and reflected. For the different samples, the values reported in Table **??** - **??** were obtained and compared with those of the same material from the literature to calculate the relative error. At least three repeatable measurements were performed for each sample, and the measurement values were averaged.

Due to the small dimensions of the specimens used in the experiments, steady-state conditions are observed for two minutes. The measurement conditions are applied in two steps. First measurement is taken prior to switching on the laser (to take into account thermal effects due to the environment outside the two spheres influencing the sensors). Then, a second measurement is made (a few minutes later) when the laser is running. This measurement represents the value of the global flux inside and outside the spheres that the sensors can identify. The difference between these two values gives us the radiant flux from the laser alone (i.e., a measurement without any thermal influence from the environment outside the two spheres). The radiant flux measurement conditions of each specimen are given in Tables **??**, **??** and **??**.

Material : Wood	Sensor positions (see Figure **??**,a.)		
Measurements (in mWm^{-2})	A	B	C
Without laser (i)	1,87	2,99	0
With laser (ii)	117,93	3,02	0
Real fluxes = (ii)-(i)	116,06	0,02	0

Table 1: Values obtained by silicon PINn (sensors) for the wood specimen

Material : Iron	Sensor positions (see Figure **??**,a.)		
Measurements (in mWm^{-2})	A	B	C
Without laser (i)	0	2,99	0
With laser (ii)	112,32	4,49	0
Real fluxes = (ii)-(i)	112,32	1,49	0

Table 2: Values obtained by silicon PINs (sensors) for the iron specimen

Material : Polycarbonate	Sensor positions (see Figure **??**,a.)		
Measurements (in mWm^{-2})	A	B	C
Without laser (i)	4,07	4,08	0,75
With laser (ii)	86,86	72,63	11,23
Real fluxes = (ii)-(i)	82,78	68,51	10,48

Table 3: Values obtained by silicon PINs (sensors) for the polycarbonate specimen

For measurements of the thermal conductivity of the specimen, the initial conditions needed to obtain the thermal steady-state condition depend strongly on the material to be studied. Tables **??** through **??** summarize the measurement values obtained for each sample material when this steady state is reached. The heat flux created by the Peltier plates that makes it possible to determine this constant varies according to the specimen studied. The wood (Table **??**) does not easily allow the flux to pass through the specimen (i.e., the wood provides good thermal insulation) unlike the iron specimen (see Table **??**), which is an excellent thermal conductor and therefore allows the heat flux to pass through the specimen quickly. Concerning the translucent material (i.e., the polycarbonate specimen), the heat flux through the material is similar to that through the wood specimen (see Tables **??** and **??**). The Polycarbonate can therefore be used for isolated construction building.

Polycarbonate					
Voltage (V)	Intensity (A)	Thickness (m)	Area (m^2)	ΔT	Flux (W)
7	0,565	0,006	0,00125664	85,5	3,955

Table 4: Polycarbonate flux and measurement data

wood					
Voltage (V)	Intensity (A)	Thickness (m)	Area (m^2)	ΔT	Flux (W)
6,7	0,565	0,005	0,00125664	94	3,7855

Table 5: Wood flux and measurement data

Iron					
Voltage (V)	Intensity (A)	Thickness (m)	Area (m^2)	ΔT	Flux (W)
12	1,8	0,007	0,00125664	1,55	21,6

Table 6: Iron flux and measurement data

4.3. Comparisons between the reference values and measurements

The total error due to the experimental device does not exceed 2%, which comprises 1% relative error contributed by all the measuring sensors and 1% relative error due to the concept of the system (i.e., the constructed McM system: the colors used, the position of the laser, the form of the system and the characteristics of the material used). For this reason, +/- 2% error is introduced for all the relative errors between the reference values and the experimental values during the comparison. Table **??** reviews these comparisons.

		K $(Wm^{-1}K^{-1})$	ρ (-)	τ (-)	α (-)
Iron	Reference	79,5	0,65	0	0,35
	Experimental (McM)	77,63	0,63	0	0,37
	Relative error (in %)	2,35	3,07	-	5,71
Wood	Reference	0,17	0,15	0	0,85
	Experimental (MCM)	0,16	0,16	0	0,84
	Relative error (in %)	5,88	1,42	-	1,23
Polycarbonate	Reference	0,22	0,12	0,82	0,06
	Experimental (McM)	0,23	0,11	0,82	0,061
	Relative error (in %)	4,54	4,75	0,56	-1,78

Table 7: Table of comparisons between the test measurements and reference values

The properties of the iron sample used as a reference have been simulated on the basis of the knowledge of the materials provided by the manufacturer: see `https://refractiveindex.info/?shelf=other&book=Ni-Fe&page=Tikuisis_bare150nm` concerning reflectance and transmittance, then `https://thermtest.com/materials-database#iron` concerning thermal conduc-

tivity (selection iron grey Cast Pearlitic (4.12C)).

The properties characterizing the wood sample used as a reference sample are given by the manufacturer Polytec (choose the reference Notaio Walnut in the list to have the value of the reflectance. The wood being opaque, does not allow light to pass through, so its transmittance is zero. We then analytically deduced the value of its optical absorbance from the formula $\alpha = 1- \rho$. Regarding the value of the thermal conductivity, a reference is given by the manufacturers on the following site (take teak wood (across grain:): `https://thermtest.com/materials-database#wood`.

The properties used to characterize the reference polycarbonate are those defined in the technical document (with the conformity test) of the following manufacturer (see page 6 for thermal conductivity and page 7 for the values of reflectance and transmittance for a 6 mm panel of model 2RS/1.3): `https://www.sunclear.fr/sites/default/files/Thermoclear_Plus_AT_6_14_2192_v1_07_2020.pdf`. The value of the reference optical absorbance is deduced analytically from the knowledge of reflectance and transmittance by $\alpha = 1- \rho - \tau$.

Our first remark is that ASTM E1225 [**?**] stipulates that a device measuring the thermal conductivity of a building material and contributing a relative error around 5% can be considered reliable. Concerning the reflectance, transmittance and absorptance, ASTM E903 [**?**] affirms that measurements of these coefficients having relative errors of less than 4% are acceptable. The McM device contributes relative errors around the ASTM values (i.e. around 5%) recommendations. Nevertheless, the CIE [**?**] illustrates the difficulty of measuring these thermal properties, and thus, the proposed devices sometimes contributes a relative measurement error of more than 5%.

Our second remark is that the experimental device is able to not only simultaneously characterize the thermo-optic-physical coefficients (i.e., absorbance, reflectance, and transmittance) of highly variable homogeneous materials and, more particularly, translucent materials (i.e., polycarbonate) but also instantly measure the value of the thermal conductivity of the same material.

Our third remark is that overall, the measurement errors of the proposed instrument are higher for the translucent material (polycarbonate) and lower for other more insulating materials (i.e. for example the wood). In general, the errors for polycarbonate are higher than the opaque materials (i.e. wood and iron).

Figure **??** illustrates the evolution of the thermal properties of each specimen.

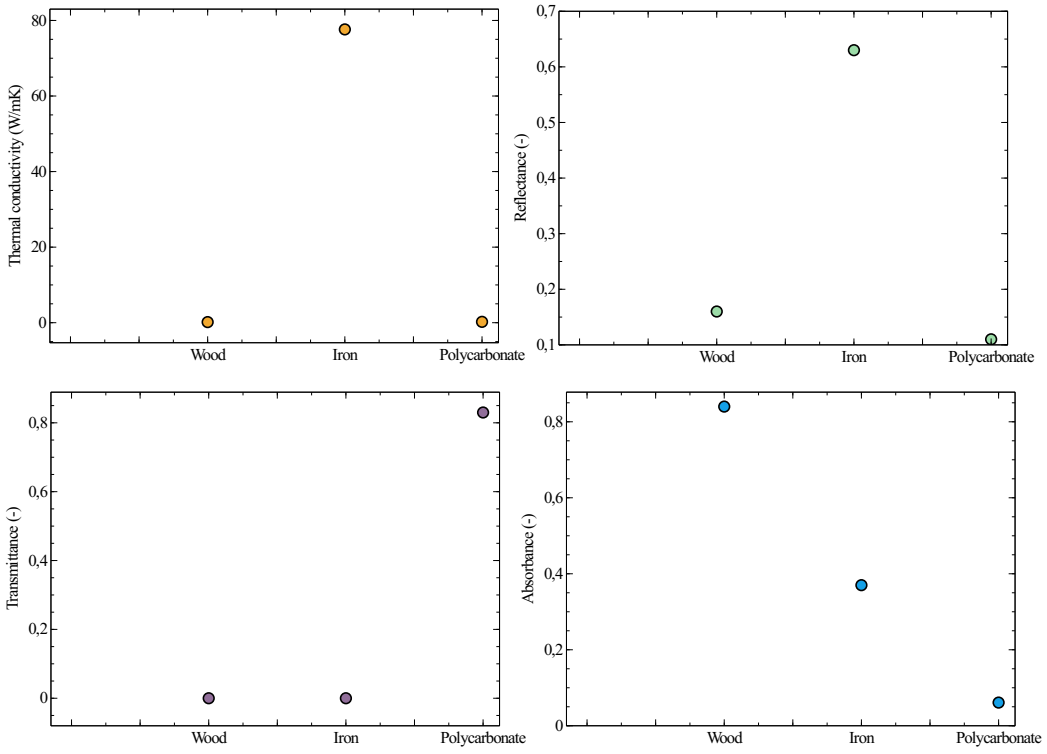

Figure 21: Thermophysical properties of the specimens studied: woood, iron and polycarbonate

Concerning the study of translucent materials, it is clear that polycarbonate can be used as thermal insulation in buildings because it has a similar thermal conductivity coefficient to that of wood (see Figure **??**). Therefore, polycarbonate has an insufficient capacity to transmit the heat that passes through it due to its low thermal conductivity (see Figure **??**). This behavior is not likely to create condensation problems in the rooms of such buildings because it has a very low absorption coefficient (see Figure **??**). The polycarbonate used in this experiment reflects very little heat (see Figure **??**) due to its light grey color. If necessary, a manufacturer could use polycarbonate with a much darker color to reflect greater amounts of heat flux and thus further reduce the heat flowing through it. This type of material is ideal for buildings in humid tropical weather zones. Polycarbonate could be used, for example, to heat a closed veranda in winter. This material can also considerably reduce the excessive moisture content on walls and ceilings.

5. Conclusions and perspectives

Scientific progress in the field of civil engineering has led to the emergence of new, peculiar thermal and optical characteristics in building materials. Currently, this is mainly the case for translucent materials. This complexity leads us to reflect on new measurement procedures that respect standard norms and perfectly satisfy the characterization of these innovated materials. This paper presents a new measuring device to simultaneously determine the values of optical and thermal coefficients (i.e., the thermal conductivity, reflectance, transmittance and absorptance

coefficients) of complex materials. The proposed device is relatively simple and economical; it is based on the theory of wave propagation in a spherical environment called an integrating sphere (a closed system). The energy source used to avoid Lambertian phenomena of flux diffusion is a monochromatic laser pointer of approximately 650 nm. The idea of a thermal flux measurement sensor based on a microphotovoltaic cell is also discussed to meet the constraints related to the positions of the measurement sensors inside the hollow sphere constituting of our experimental device. These sensors have been specially calibrated through comparison with a reference fluxmeter exposed to the same monochromatic source (laser). In this research, we propose a new protocol adapted to this measurement system. The experimental measurement results obtained show that the innovative device has an overall error of around 5% (which is acceptable for a machine that measures heat fluxes according to the ASTM standard recommendation) and has a maximum energy source power reaching up to 200 mW.

Since the beginning of the 20th century, research has been carried out to develop an instrument capable of simultaneously measuring the transmittance, absorptivity and reflectance of a material regardless of whether it is opaque, transparent or translucent. This process, in addition to being very challenging mathematically, has been very expensive because when it has been implemented experimentally, two integrating spheres and high-precision detectors were used, but they were excessively expensive; besides, the spheres and detectors were very laborious to manufacture.

Another disadvantage that arose was that the instrumentation allowed the measurement of the thermophysical properties of materials with certain dimensions only.

In the present study, these disadvantages are alleviated through the use of low-cost materials as well as a novel method of measuring the properties of materials with different dimensions.

Another advantage that we achieve with this configuration is the possibility of measuring the conductivity and diffusivity by simply making a few small adjustments.

In the future, it would be interesting to modify the experimental setup to study the thermal diffusivity of complex materials.

Similarly, a study should be conducted to propose a low-cost and straightforward experimental system capable of measuring all the thermophysical properties of a liquid or gaseous substance simultaneously.

Acknowledgement

The authors would like to thank Professor Antonio Parretta (University of Ferrara in Italy) for his valuable advice on this work as well as the European project ERASMUS+ for the financial support of this research project through internship grants.

Appendix A

Laser features	
Wavelength	650 nm
Output power	200 mW
Useful life	5000-8000 hours
Point size	<18 mm of 10 m
USB interface	Andrews 2.0
Housing material	aeronautical aluminum
Surface treatment	oxidation treatment, rubber painting
Electronic protection	PCB protection, reverse polarity protection
Waterproofing standard	IPX4
Operating current	<320 mA
Operating voltage	DC=3.7 V
Operating temperature	$5°C$ - 50°
Net weight	80 g
Dimensions	20 x 140 mm

Table A. Laser features

Appendix B

Performance specifications TEC1-12706		
Hot-side temperature (°C)	25°C	50°C
Qmax (Watts)	50	57
Delta Tmax (°C)	66	75
Imax (Amps)	6.4	6.4
Vmax (Volts)	14.4	16.4
Module resistance (Ohms)	1.98	2.30
Dimensions	40 mm X 40 mm X 3.8 mm	

Table B. Performance specifications TEC1-12706

Appendix C

Propierties CSEC3

The CSEC Series encompasses an economic range of temperature calibration sources and is available in three versions, each of which provides a highly accurate, very stable temperature output that is ideal for the calibration of probe thermometers as well as general-purpose temperature measuring instruments.

- To use with probe thermometers
- Standard front 7-hole probe insert
- PID controller with platinum film sensor
- High accuracy and stable temperature source
- User-adjustable temperature
- User-adjustable °C or °F display

The CSEC3 Series covers a temperature range from -30.0°C below the ambient temperature (min -10°C) to +105.0°C.